

TIME-RESOLVED X-RAY DIFFRACTION STUDIES ON THE  
INTENSITY CHANGES OF THE 5.9 AND 5.1 NM ACTIN  
LAYER LINES FROM FROG SKELETAL MUSCLE DURING  
AN ISOMETRIC TETANUS USING  
SYNCHROTRON RADIATION

KATSUZO WAKABAYASHI,\* HIDEHIRO TANAKA,‡ YOSHIYUKI AMEMIYA,§ AKIRA FUJISHIMA,\*  
TAKAKAZU KOBAYASHI,‡ TOSHIKI HAMANAKA,\* HARUO SUGI,‡ AND TOSHIO MITSUI\*  
\*Department of Biophysical Engineering, Faculty of Engineering Science, Osaka University, Toyonaka,  
Osaka, Japan 560; ‡Department of Physiology, School of Medicine, Teikyo University, Itabashi-ku,  
Tokyo, Japan 173; and §Photon Factory, National Laboratory for High Energy Physics, Oho-machi,  
Tsukuba-gun, Ibaraki, Japan 305

**ABSTRACT** Time-resolved x-ray diffraction studies have been made on the 5.9- and 5.1-nm actin layer lines from frog skeletal muscles during an isometric tetanus at 6°C, using synchrotron radiation. The integrated intensities of these actin layer lines were found to increase during a tetanus by 30–50% for the 5.9-nm reflection and ~70% for the 5.1-nm reflection of the resting values. The intensity increase of both reflections was greater than that taking place in the transition from rest to rigor state. The intensity change of the 5.9-nm reflection preceded those of the myosin 42.9-nm off-meridional reflection and of the equatorial reflections, as well as the isometric tension development. The intensity profile of the 5.9-nm layer line during contraction was found to be different from that observed in the rigor state.

In the x-ray diffraction patterns from striated muscles, the 5.9- and 5.1-nm layer-line reflections arise only from the thin filaments because of different periodicities between the thick and thin filaments. They correspond to the pitches of the left-handed and right-handed one-start helices of the F-actin filament, respectively. The intensities of these layer lines are related to the electron density distributions of actin in the thin filament projected onto the respective helices, being sensitive to the shape and orientation of actin in the filament (1–5). In 1975, Haselgrove (6) reported that there was a slight increase in the intensity of the 5.9- and 5.1-nm actin layer lines during contraction of frog skeletal muscle. However, he paid little attention to these changes because of a large uncertainty in measuring the layer-line intensities.

To obtain clues about the actin-myosin interaction during muscle contraction, we examined the intensity changes of the 5.9- and 5.1-nm actin layer lines when frog skeletal muscles were tetanized isometrically, using intense x-rays of synchrotron radiation from the storage ring at the Photon Factory, Tsukuba, Japan. The results presented

here show that there are genuine intensity increases of these actin layer lines during a tetanus, that their intensity profiles are different from that of rigor muscle, and that their changes precede the intensity changes of the myosin 42.9-nm reflection and the equatorial reflections as well as the isometric tension development.

The sartorius muscle of bullfrog (*Rana catesbeiana*) was mounted vertically in a specimen chamber with a multi-electrode assembly. The pelvic end of the muscle was clamped to the chamber while the tibial end was connected to a force transducer (model UT; Shinkoh Co., Tokyo Japan). The sarcomere length of muscles was adjusted to ~2.4  $\mu\text{m}$  using the optical diffraction of He-Ne laser light. The muscle was continuously perfused with oxygenated Ringer's solution (6°C, 115 mM NaCl, 2.5 mM KCl, 1.8 mM CaCl<sub>2</sub>, pH adjusted to 7.2 with NaHCO<sub>3</sub>) and stimulated with trains of 3-ms supramaximal current pulses at 25–30 Hz to produce isometric tetani. Each muscle was tetanized 20 times at intervals of 15 s. Tension was monitored and recorded with a storage oscilloscope (5110; Tektronix, Inc., Beaverton, OR).

A focused and monochromatized x-ray beam of wavelength 1.5 Å was produced by a camera designed by Amemiya et al. (7) from the synchrotron radiation of the

Correspondence should be addressed to Dr. Wakabayashi.

storage ring operated at an energy of 2.5 GeV, with the beam current between 50 and 150 mA. The camera consisted of seven, 20 cm long segments of totally reflecting curved silica mirror and a bent triangular-shaped silicon crystal monochromator cut at  $7.8^\circ$  to the 111 planes (8). The specimen-to-detector distance was 240 cm, and the beam sizes at the specimen and at the detector plane were  $2 \text{ mm} \times 5 \text{ mm}$  and  $1.3 \text{ mm} \times 2.6 \text{ mm}$  (vertical  $\times$  horizontal), respectively. The diffraction pattern was recorded with a 20 cm long, linear position-sensitive detector using a 400-ns internal delay line (Rigaku Denki Co., Tokyo) and an encoding digitizer (4202; LeCroy Research Systems S.A., Geneva, Switzerland) for position readout. The signals of one-dimensional patterns were stored as a function of time in a CAMAC memory (3588; LeCroy Research Systems S.A.) linked to a computer (micro-11/F23; Automation System Research, Tokyo, Japan). The memory was divided into 64 segments of 256 channels, each corresponding to a successive time frame of data collection. Data over 20 tetani for each muscle were accumulated in the relevant memory segment, and the results from different muscles were added to obtain the intensity with reasonable counting statistics.

Fig. 1 shows an example of the time-resolved diffraction diagrams of off-meridional reflections during isometric tetani. The peaks of the 5.9- and 5.1-nm layer-line reflections lie at slightly different radial positions and the detector was placed with its long axis parallel to the meridian at the position between them. In this case, the whole period (3 s) of each experiment was divided into 30

frames of 100-ms duration. Stimulation was started at the 5th frame and ceased at the 20th frame. In Fig. 1, the inner five reflections correspond to the subsidiary peaks on the myosin layer lines that are indexed to the second, third, fourth, fifth, and sixth order of the 42.9-nm periodicity, whereas the two outermost ones correspond to the 5.9- and 5.1-nm actin reflections. During isometric tension development, the intensities of both actin reflections were found to increase, whereas the widths of these reflections in the axial direction tended to decrease; in particular, the width of the 5.9-nm reflection decreased by 10–15% of the resting value. On the other hand, all the subsidiary peaks on myosin layer lines decreased their intensity during the tension development, but they did not disappear completely (see Huxley et al. [9, 10]). The intensity decrease of these myosin reflections has been attributed to a rearrangement of the myosin projections occurring on activation. On cessation of stimulation, the intensities of both actin and myosin reflections started to return towards their original resting levels.

To record the changes of profiles and the overall intensities of the 5.9- and 5.1-nm layer lines, the detector was placed with its long axis perpendicular to the meridian at the position of each layer line. To avoid the intrusion of the nearby myosin layer lines (9), the size of the entrance slit placed in front of the detector was 3.5 mm wide  $\times$  180 mm long. The detector of this length covered the range of  $R \approx 0.26 \text{ nm}^{-1}$  across the meridian (where  $R$  denotes the reciprocal space radial coordinate), including the main off-meridional profiles. Though the 5.9-nm layer line is

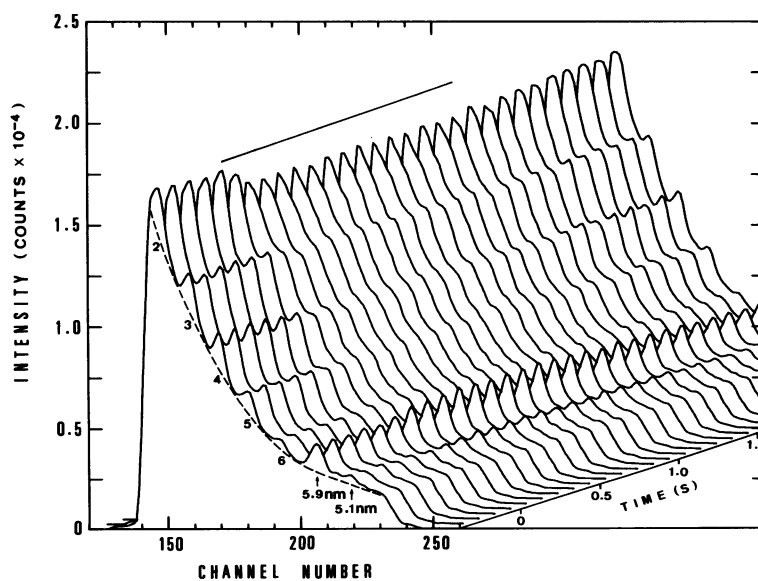


FIGURE 1 Time-resolved x-ray diffraction diagrams of the off-meridional reflections during an isometric tetanus at  $6^\circ\text{C}$ . Data were taken by placing the detector with its long axis parallel to the meridian. A slit 10 mm wide was used in front of the detector so that the detector covered the radial region of  $0.05 \text{ nm}^{-1} \leq R \leq 0.07 \text{ nm}^{-1}$ . The whole period (3 s) of each experiment was divided into 30 frames of 100-ms duration. Tetani were repeated 20 times and the data from six different muscles were added. The total exposure time for each curve was 12 s. The 5.9- and 5.1-nm actin reflections are indicated by arrows. The peaks indicated by 2–6 are the myosin off-meridional reflections corresponding to the second to sixth order of the 42.9-nm periodicity. The broken curve in the first frame denotes the estimated background. The bar on the diagram indicates a period of stimulation.

broadened in its axial direction, we confirmed that the detector collected most of the total intensity ( $\sim 80\%$ ) of this reflection as recorded on film from resting muscles. As was done by Yagi et al. (11), the background was determined by densitometer tracing of the diffraction patterns recorded on film from resting muscles. Scannings were made perpendicular to layer lines at intervals of 1 mm across the positions of the slit aperture. For each trace, the background curve was drawn to levels seen between the successive layer-line peaks (such as a broken curve in Fig. 1). The signal-to-background ratios in the regions of the detector that receive x rays through the slit were calculated as a function of the  $R$  coordinate. The background was then determined by multiplying the signals taken with the detector by these ratios. Fig. 2 shows the intensity distribu-

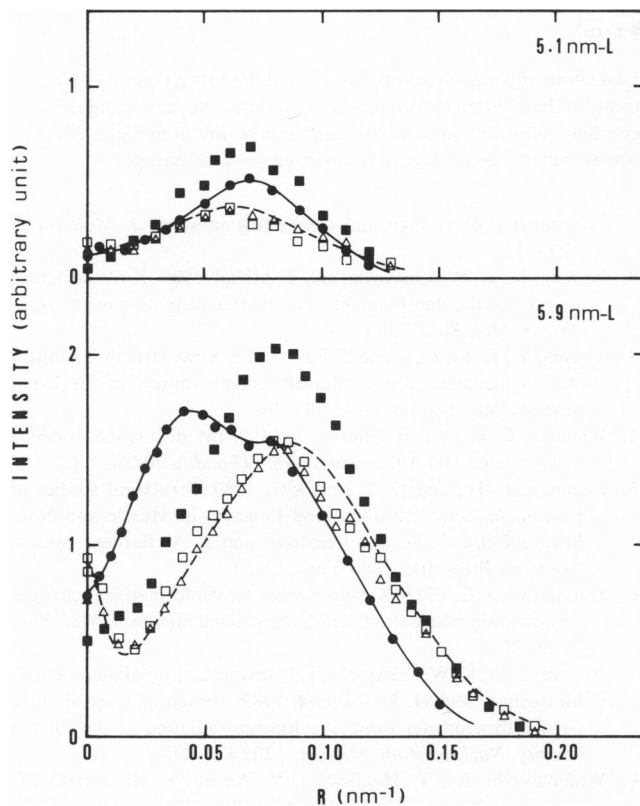


FIGURE 2 Change in the intensity profiles of the 5.9- and 5.1-nm actin layers lines. Data were taken by setting the detector with its long axis perpendicular to the meridian. The size of the slit in front of the detector was 3.5 nm wide  $\times$  180 mm long so that the detector covered the range of  $R \lesssim 0.26 \text{ nm}^{-1}$  across the meridian, including the main off-meridional profiles. The other condition was the same as in Fig. 1. The patterns at rest ( $\square$ ), during the plateau of an isometric tetanus ( $\blacksquare$ ), and at the end of relaxation ( $\triangle$ ) are shown. Data from nine muscles were added so that the total exposure time for these patterns was 18 s. Dashed and solid curves denote the intensity profiles of the same muscles in living relaxed and rigor states, respectively, taken for the same exposure time by photographic films with the laboratory x-ray source (FR-B; Rigaku Denki Co.). The rigor muscles were made following the procedure of Huxley and Brown (9). Intensity data by photographic recording and by the detector recording were normalized with respect to the integral values of the 5.9-nm reflection at rest.

tions of these actin layer lines after subtracting the background. The open squares, solid squares, and triangle symbols represent the patterns recorded at rest, at the plateau of a tetanus, and at the end of relaxation, respectively. It can be seen that these actin layer lines increase their intensity, and the profile of the 5.9-nm layer line spreads slightly towards the meridian during contraction, and returns to the resting value at the end of relaxation. As reported by Huxley and Brown (9) and Haselgrove (6), the intensity profile of the 5.9-nm layer line shifted towards the meridian when muscles were put into rigor state (the solid-line curve in Fig. 2). It was very different from the profile observed during contraction. In the 5.9-nm layer line, a weak but distinct reflection can be seen on the meridian at virtually the same axial spacing as the off-meridional reflection (9); its intensity was observed to decrease during contraction and to return towards the resting value during relaxation, like the behavior of the myosin off-meridional reflections. This reflection disappeared in the rigor state. The occurrence of this meridional reflection has been discussed by Egelman et al. (4, 5) in relation with the axial perturbation of the structure of actin monomer in the filament. The integrated intensity (the area under the profile) of the 5.9-nm layer line was found to increase by  $\sim 30\text{--}50\%$  of the resting value during the plateau of tetanic tension. Though it was difficult at present to accurately measure the change of the intensity distribution of the 5.1-nm layer line because it was diffuse and much weaker than the 5.9-nm layer line, our preliminary measurements indicated that the relative increase of its intensity was greater than the 5.9-nm layer line;  $\sim 70\%$  increase of the resting value. In our measurement shown in Fig. 2, increase of the integrated intensities of both reflections was greater than the intensity increase ( $\sim 15\%$ ) that took place by transition from rest to rigor state.

When the sarcomere length of the muscle was stretched to  $\sim 2.9 \mu\text{m}$ , the intensity changes of both reflections during contraction were reduced, but the amount of intensity increase was greater for the 5.9-nm reflection than for the 5.1-nm one; an increase relative to the rest value of  $\sim 25\%$  for the 5.9-nm reflection and  $< 15\%$  for the 5.1-nm reflection.

There is very little sign of a lattice sampling effect on these actin layer lines (4, 5, 9). In Fig. 2, the radial extent of the 5.9-nm reflection at rest and during contraction corresponds to that to be expected from independent diffractors  $\sim 10 \text{ nm}$  wide (4). This result indicates that the binding of myosin projections to actin during an isometric tetanus does not produce a change of intensity distribution of the 5.9-nm reflection like that taking place during the transition from rest to rigor.

In Fig. 3, the time course of change in the integrated intensity of the 5.9-nm reflection is shown with a time resolution of 10 ms, together with those of the 42.9-nm myosin off-meridional reflection, the 1,0 and 1,1 equatorial reflections, and the isometric tension. They are plotted as a

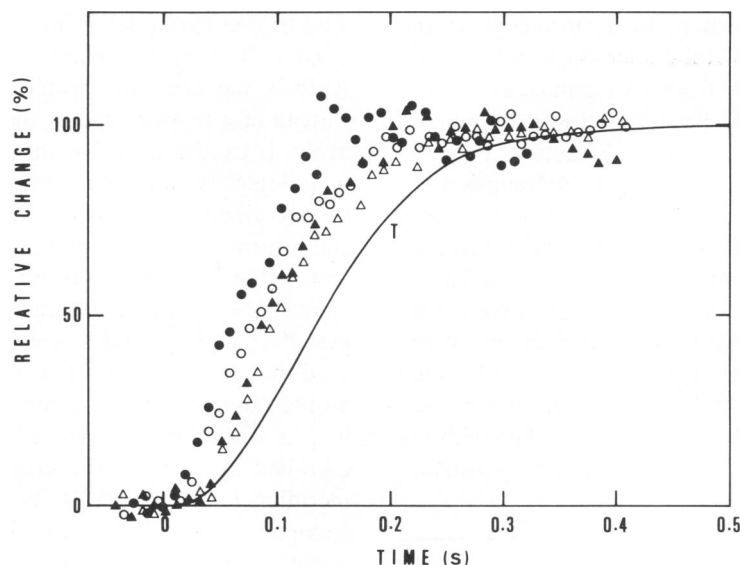


FIGURE 3 Time course of the intensity changes of the 5.9-nm actin (●), the 42.9-nm myosin off-meridional (○), and the 1,0 (△) and 1,1 (▲) equatorial reflections together with the isometric tension (curve *T*). The intensity of the 42.9-nm reflection was measured at the radial range of  $0.039 \text{ nm}^{-1} \leq R \leq 0.061 \text{ nm}^{-1}$ , corresponding to the strongest part of this layer line. Actin data were taken along the layer line as in Fig. 2. All data are taken with 10-ms time resolution, the average of 10 muscles, and are plotted as a percentage of the average maximal change.

percentage of their average maximal changes against time after stimulation. The intensity change of the 5.9-nm reflection reached its maximum earlier than not only the isometric tension development, but also the intensity changes of the 42.9-nm reflection and the equatorial reflections; the point of half-maximum change is reached  $\sim 70$  ms ahead of half-maximum tension,  $\sim 20$  ms ahead of the half-maximum changes of the 42.9-nm reflection and the equatorial reflections. As shown in Fig. 3, the intensity of the 5.9-nm reflection tended to decrease after reaching the maximum value. The intensity change of the 5.1-nm reflection also proceeded with a time course similar to that of the 5.9-nm reflection. These results suggest that the intensity change of the actin layer lines reflects the first step of structural changes leading to contraction.

During the preparation of this paper, we became aware of the report of Kress et al. (12) on the intensity change of the actin layer lines during contraction of frog skeletal muscles. Their results are basically similar to ours.

We thank Drs. H. Hashizume of the Tokyo Institute of Technology and T. Wakabayashi of the University of Tokyo, and Professors K. Kohra and T. Sasaki of the Photon Factory, National Laboratory for High Energy Physics, Tsukuba, Japan for their encouragement. Thanks are also due to Drs. N. and K. Sakabe and K. Sasaki of Nagoya University for their kind help in using a drum-scan microdensitometer. K. Wakabayashi is indebted to Professor F. Oosawa of Osaka University for stimulating discussions.

Received for publication 29 November 1984 and in final form 11 February 1985.

#### REFERENCES

1. Parry, D. A. D., and J. M. Squire. 1973. Structural role of tropomyosin in muscle regulation: analysis of x-ray diffraction patterns from relaxed and contracting muscles. *J. Mol. Biol.* 75:33-55.
2. Namba, K., K. Wakabayashi, and T. Mitsui. 1980. X-ray structure analysis of the thin filament of crab striated muscle in the rigor state. *J. Mol. Biol.* 138:1-26.
3. Tajima, Y., K. Kamiya, and T. Seto. 1983. X-ray structure analysis of thin filaments of a molluscan smooth muscle in the living relaxed state. *Biophys. J.* 43:335-343.
4. Egelman, E. H., and R. Padrón. 1984. X-ray diffraction evidence that actin is a 100 Å filament. *Nature (Lond.)* 307:56-58.
5. Egelman, E. H., and D. J. DeRosier. 1983. Structural studies of F-actin. In *Actin: Structure and Function in Muscle and Non-Muscle Cells*. C. G. dos Remedios and J. A. Barden, editors. Academic Press, Inc., New York. 17-23.
6. Haselgrove, J. C. 1975. X-ray evidence for conformational changes in the myosin filaments of vertebrate striated muscle. *J. Mol. Biol.* 75:33-55.
7. Amemiya, Y., K. Wakabayashi, T. Hamanaka, T. Wakabayashi, T. Matsushita, and H. Hashizume. 1983. Design of a small-angle x-ray diffractometer using synchrotron radiation at the Photon Factory. *Nucl. Instrum. Methods.* 208:471-477.
8. Wakabayashi, K., T. Hamanaka, Y. Amemiya, H. Tanaka, T. Wakabayashi, and H. Hashizume. 1983. Performance of the muscle diffractometer. In *Photon Factory Activity Report 1982/83*, National Laboratory for High Energy Physics, Tsukuba. VI88-90.
9. Huxley, H. E., and W. Brown. 1967. The low-angle x-ray diagram of vertebrate striated muscle and its behavior during contraction and rigor. *J. Mol. Biol.* 30:383-434.
10. Huxley, H. E., A. R. Faruqi, M. Kress, J. Bordas, and M. H. J. Koch. 1982. Time-resolved x-ray diffraction studies of the myosin layer-line reflections during muscle contraction. *J. Mol. Biol.* 158:637-684.
11. Yagi, N., E. J. O'Brien, and I. Matsubara. 1981. Changes of thick filament structure during contraction of frog striated muscle. *Biophys. J.* 33:121-138.
12. Kress, M., H. E. Huxley, A. R. Faruqi, M. H. J. Koch, and J. Hendrix. 1984. Thin filament x-ray diffraction in contracting frog muscle. In *The Eighth International Biophysics Congress Abstracts*, Bristol. 119.